Protein Science (2000), *9*:1053–1062. Cambridge University Press. Printed in the USA.

Stereoselectivity of *Pseudomonas cepacia* lipase toward secondary alcohols: A quantitative model

TANJA SCHULZ, JÜRGEN PLEISS, AND ROLF D. SCHMID

Institute of Technical Biochemistry, University of Stuttgart, Allmandring 31, D-70569 Stuttgart, Germany

(RECEIVED October 13, 1999; FINAL REVISION January 21, 2000; ACCEPTED March 20, 2000)

Abstract

The lipase from *Pseudomonas cepacia* represents a widely applied catalyst for highly enantioselective resolution of chiral secondary alcohols. While its stereopreference is determined predominantly by the substrate structure, stereoselectivity depends on atomic details of interactions between substrate and lipase. Thirty secondary alcohols with published E values using *P. cepacia* lipase in hydrolysis or esterification reactions were selected, and models of their octanoic acid esters were docked to the open conformation of *P. cepacia* lipase. The two enantiomers of 27 substrates bound preferentially in either of two binding modes: the fast-reacting enantiomer in a productive mode and the slow-reacting enantiomer in a nonproductive mode. Nonproductive mode of fast-reacting enantiomers was prohibited by repulsive interactions. For the slow-reacting enantiomers in the productive binding mode, the substrate pushes the active site histidine away from its proper orientation, and the distance $d(H_{N\epsilon} - O_{alc})$ between the histidine side chain and the alcohol oxygen increases. $d(H_{N\epsilon} - O_{alc})$ was correlated to experimentally observed enantioselectivity: in substrates for which *P. cepacia* lipase has high enantioselectivity ($E > 100$), $d(H_{N\epsilon} - O_{alc})$ is >2.2 Å for slow-reacting enantiomers, thus preventing efficient catalysis of this enantiomer. In substrates of low enantioselectivity ($E < 20$), the distance $d(H_{N\epsilon} - O_{alc})$ is less than 2.0 Å, and slow- and fast-reacting enantiomers are catalyzed at similar rates. For substrates of medium enantioselectivity ($20 < E < 100$), $d(H_{N\epsilon} - O_{alc})$ is around 2.1 Å. This simple model can be applied to predict enantioselectivity of *P. cepacia* lipase toward a broad range of secondary alcohols.

Keywords: enantioselectivity; lipase; model; molecular dynamics; *Pseudomonas cepacia*; secondary alcohol; stereopreference

Lipase from *Pseudomonas cepacia* (EC 3.1.1.3) is a popular catalyst in organic synthesis (Kazlauskas & Bornscheuer, 1998) for the kinetic resolution of racemic mixtures of secondary alcohols in hydrolysis (Laumen & Schneider, 1988; Liang & Paquette, 1990; Caron & Kazlauskas, 1991; Schneider & Georgens, 1992; Bänziger et al., 1993; Itoh et al., 1993; Partali et al., 1993; Takano et al., 1993; Waldinger et al., 1996), esterification (Burgess & Jennings, 1991; Uejima et al., 1993; Chadha & Manohar, 1995; Gaspar & Guerrero, 1995; Hamada et al., 1996; Petschen et al., 1996), and transesterification (Kaminska et al., 1996; Takagi et al., 1996). The mechanistic details of the catalytic reaction of serine hydrolases (Chapus et al., 1976; Chapus & Sémériva, 1976) have been well investigated by quantum-chemical methods like the ab initio and density functional theory (Hu et al., 1998), and by semiempirical methods (Monecke et al., 1998). The reaction mechanism of ester hydrolysis (Fig. 1) starts with the formation of a Michaelis complex followed by a first transition state (1′) to the first tetrahedral intermediate (2), where the substrate is covalently linked to side-chain oxygen Oγ of catalytic serine. The crucial hydrogen bonds from $H_{n\epsilon}$ of catalytic histidine to serine Oγ and the oxygen of the alcohol moiety are formed. Transfer of $H_{N\epsilon}$ to the oxygen of the alcohol moiety splits away the alcohol and an acyl–enzyme complex is formed (3), which is then hydrolyzed by water to the second tetrahedral intermediate (4). Quantum-chemical methods identified the transition state (2′) that initiates the breakdown of the first tetrahedral intermediate as crucial reaction step (Ema et al., 1998).

X-ray structures of *Candida rugosa* lipase complexes with enantiomeric inhibitors showed the structural basis for chiral recognition of secondary alcohols (Cygler et al., 1994). The different interactions of the two enantiomers with the lipase resulted in a conformational change of the catalytic histidine, preventing efficient catalysis of analogues slow-reacting enantiomers of substrates. MNDO-PM3 calculations (Ema et al., 1998) also showed the tendency of slow-reacting enantiomers to disturb the orientation of catalytic histidine and the surrounding hydrogen-bonding network, thus resulting in severe lipase-induced strain at the transition state, compared to fast-reacting enantiomers.

Based on the observed selectivity in lipase-catalyzed conversions of secondary alcohols and on mechanistic details, models to

Reprint requests to: Rolf D. Schmid, Institute of Technical Biochemistry, University of Stuttgart, Allmandring 31, D-70569 Stuttgart, Germany; e-mail: Rolf.D.Schmid@rus.uni-stuttgart.de.

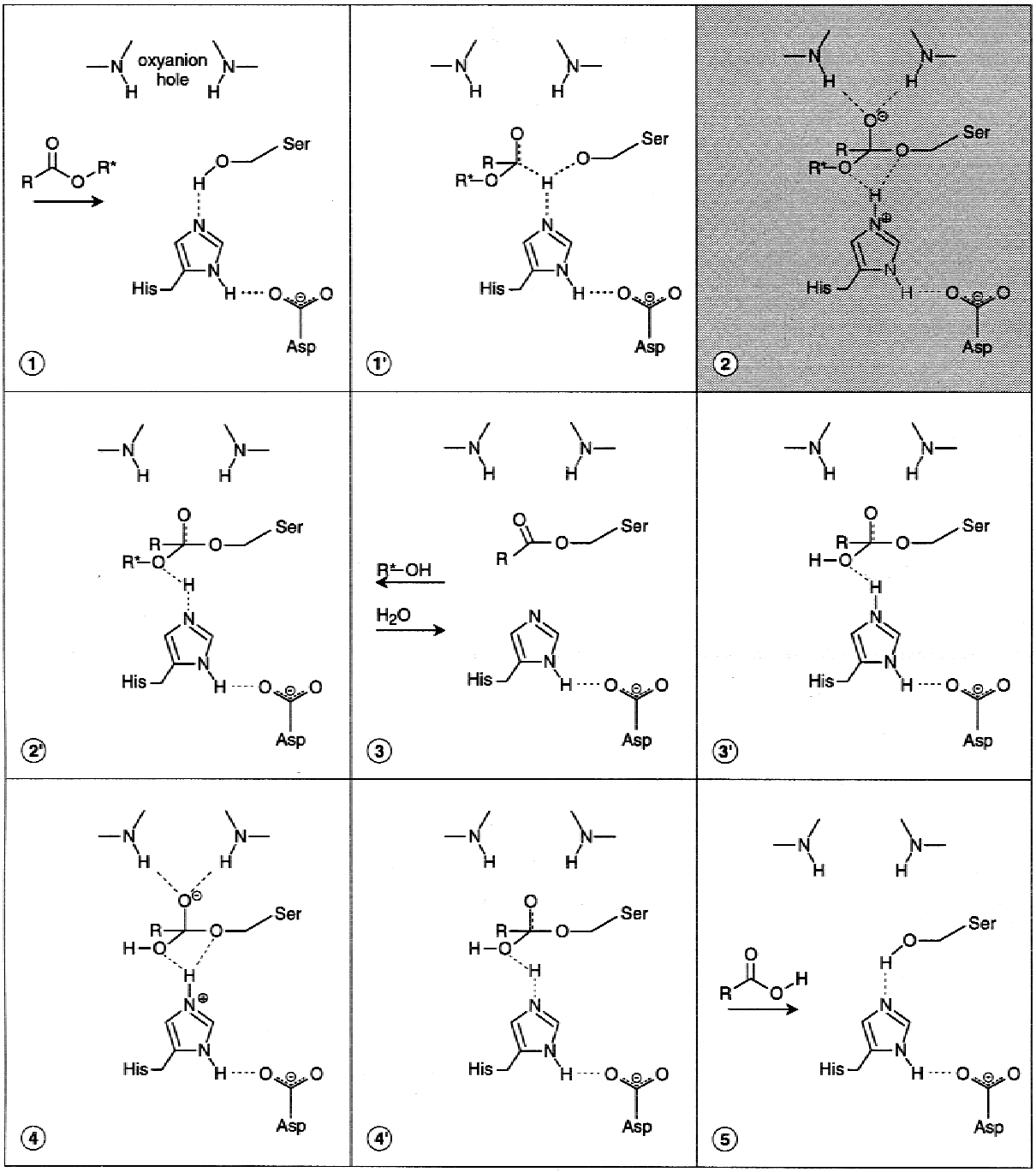

Fig. 1. Educts, products, intermediates (1, 2, 3, 4, 5), and transition states (1′, 2′, 3′, 4′) of lipase-catalyzed hydrolysis of secondary alcohols (R = acid chain and R* = secondary alcohol part). Partial reactions of the enzymatic hydrolysis are attack of the ester (1′), cleavage of the alcohol (2′), attack of the water (3′), and cleavage of the acid (4′). The modeled intermediate (2) is shaded gray.

predict stereopreference were developed. A reliable empirical rule for all lipases was proposed (Kazlauskas et al., 1991), which is simply based on a classification of the relative size of the substituents at the stereocenter of the secondary alcohol. Effects on enantioselectivity of substituent modification were investigated experimentally by modifying the size of the large (Rotticci et al., 1997) (*Candida antarctica* lipase B) and the medium-sized substituent (Shimizu et al., 1992). Investigations on size limits (Burgess & Jennings, 1991; Naemura et al., 1994, 1995) (*Pseudomonas fluorescens* lipase) and of electronic effects (Hönig et al., 1994) (*P. cepacia* lipase) of the substituents have also been reported. However, the quantitative effects of substrate modifications on enantioselectivity are still not predictable.

Attempts to calculate enantioselectivity using force-field methods have been made (DeTar, 1981; Bemis et al., 1992; Faber et al., 1994; Orrenius et al., 1998), for example, calculations of energy

differences using molecular dynamics and molecular mechanics of substrate–lipase complexes have been successfully used to predict stereopreference. However, the calculated values of potential energy differences between the diastereomeric substrate–lipase complexes did not correlate with experimental enantioselectivity (Haeffner et al., 1998).

To circumvent the limitations of free energy and entropy calculations, we combined flexible docking based on structural information of inhibited lipase from *P. cepacia* (Lang et al., 1998) with a ranking strategy, which evaluates geometrical properties of the enzyme–substrate complexes and correlated them to experimentally determined enantioselectivity E.

Results

Substrates and classification of substituents

Thirty octanoic acid esters of secondary alcohols (Fig. 2) were investigated, which differed over a wide range of enantioselectivity in *P. cepacia* lipase catalyzed conversion (Kazlauskas & Bornscheuer, 1998). Secondary alcohols consist of two substituents of different size at the stereocenter: a large substituent (L) and a medium-sized substituent (M). The investigated substrates varied in physicochemical properties of these two substituents. For each investigated substrate, both enantiomers were evaluated. They were classified as fast- and slow-reacting enantiomers (Kazlauskas et al., 1991).

Binding pockets

For all investigated substrates, the fatty acid chain was docked to the *hydrophobic crevice* (Fig. 3). The oxyanion of the tetrahedral substrate–lipase intermediate was placed within the oxyanion hole, which is composed of residues L17 and Q88. Further binding pockets to which a secondary alcohol moiety could bind (Fig. 3) were identified by docking studies using molecular dynamics simulations and characterized by their size, shape, and physicochemical properties:

1. The *hydrophobic dent* is a large, shallow, hydrophobic binding pocket with a diameter of 4.3 Å, formed by side chains of

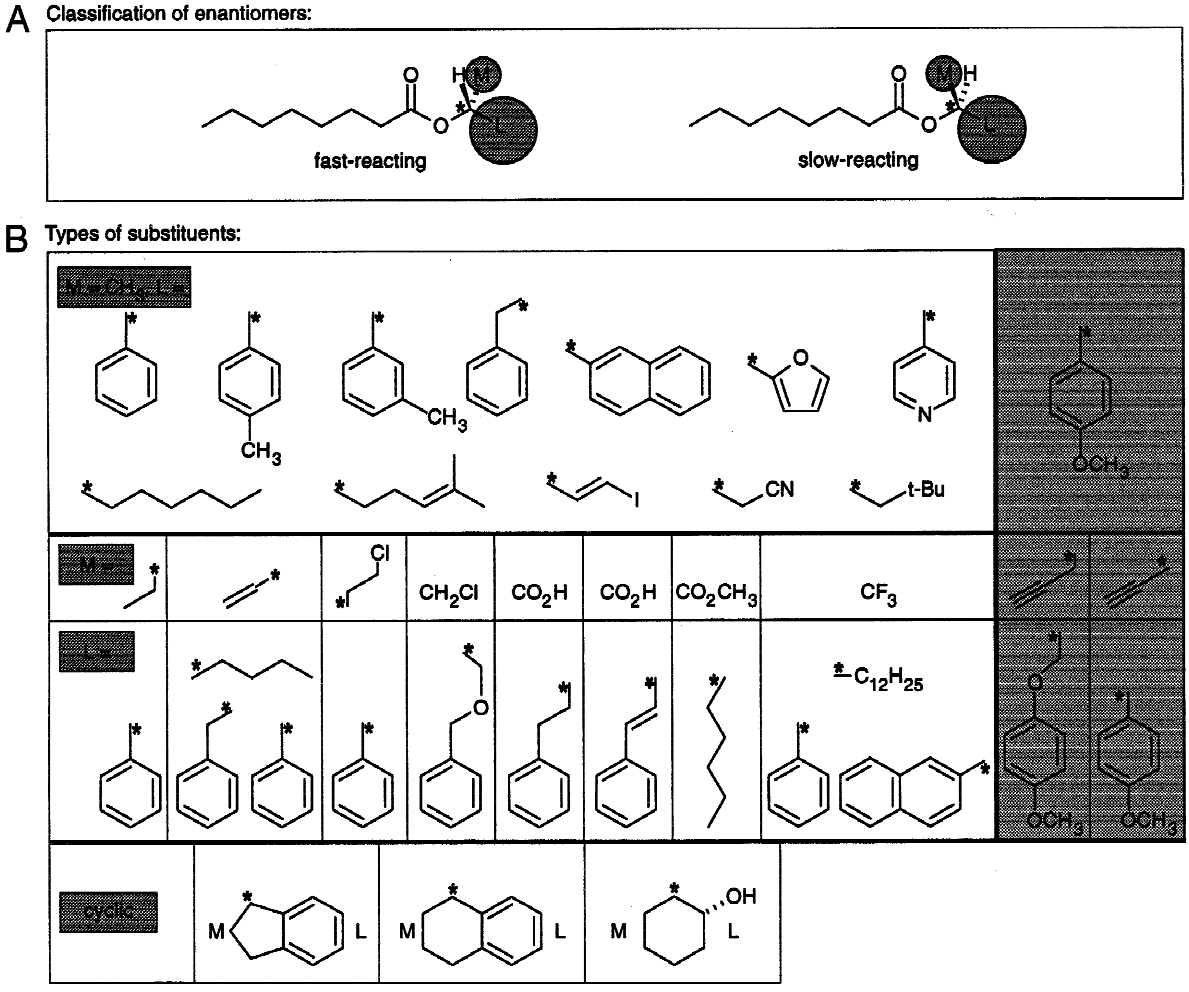

Fig. 2. A: Classification in fast- and slow-reacting enantiomers in lipase catalyzed conversions (Kazlauskas et al., 1991). **B:** Substituents (*M* = medium-sized substituent and *L* = large substituent) of investigated substrates in the conversion of secondary alcohols catalyzed by *P. cepacia* lipase. The carbon at the stereocenter is indicated with an *. The three outliers in Figure 5B are shaded gray.

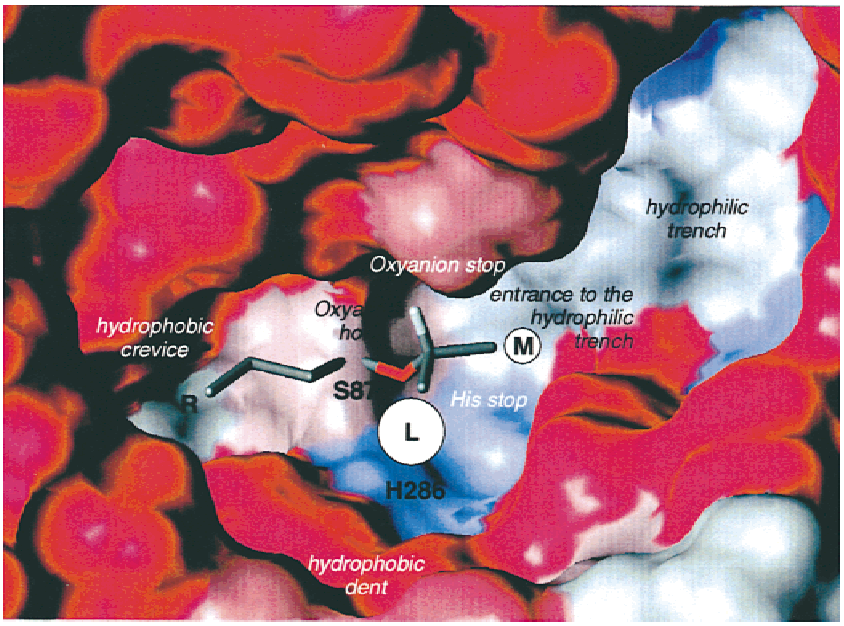

Fig. 3. Calculated surface of the alcohol binding site of *P. cepacia* lipase, colored by physico-chemical properties (blue—polar, red—hydrophobic) including a fast-reacting enantiomer (capped sticks). Substituents at the stereocenter of the secondary alcohol are abbreviated with *M* for the medium-sized substituent, *L* for the large substituent, and *R* represents the fatty acid chain. Atom colors of substrate atoms are gray for carbon and red for oxygen atoms. The hydrogen atom at the stereocenter is displayed and colored white.

residues L248, L287, and V266, and backbone atoms of catalytic H286. Due to its size and hydrophobicity, this pocket is appropriate to bind a large, hydrophobic substituent.

2. The *entrance to the hydrophilic trench* is a sphere of 4.5 Å in diameter, of medium hydrophobicity and composed of side chains of residues T18, Y29, H86, L287, and I290. It preferentially binds the medium-sized substituent of the secondary alcohols. Side chains at the entrance to the hydrophilic trench adjust well to the shape of the medium-sized substituent. The entrance is separated from the hydrophilic trench by a *contraction* composed of the side chains of residues Y29 and L287, the latter being the C-terminal neighbor of catalytic H286.

3. Medium-sized substituents of investigated secondary alcohols are not large enough to reach the hydrophilic trench. Thus, this binding pocket plays no crucial role in the investigated binding modes of secondary alcohols.

In addition to these binding pockets, two rigid *stops* are present, which limit the size of the binding site within *P. cepacia* lipase:

1. The *oxyanion stop* is situated next to the oxyanion hole close to the alcohol moiety and is composed of rigid backbone atoms of L17 and neighboring T18. Atoms at the stereocenter other than hydrogen atoms cause repulsive interactions, when they point toward the oxyanion stop.

2. The *His stop* is near to the hydrophobic dent and composed of side chains of H86 and catalytic H286 as well as of backbone atoms of H286. It is favorable to place the hydrogen atom at the stereocenter directing toward this stop.

Whether the oxyanion stop or the His stop interacts with hydrogen atoms or substituents at the stereocenter depends on the binding mode.

Geometry of the substrate–lipase complexes (binding modes)

Due to geometric constraints of a secondary alcohol, its physico-chemical properties, size, shape, and position in the lipase binding site, and the localization of binding pockets in the binding site of *P. cepacia* lipase, the number of possible orientations of a substrate is limited. During molecular dynamics simulation, the side-chain geometry of the lipase and the conformation of the substrate adapted; in some cases the substrate underwent a conformational change. Finally, two preferred geometries of substrates within the lipase binding site (binding modes) were obtained (Fig. 4).

Binding mode I (productive)

Binding mode I is characterized by a short distance between the hydrogen atom $H_{N\epsilon}$ of catalytic H286 and the alcohol oxygen of the substrate O_{alc}. Because $d(H_{N\epsilon} - O_{alc})$ is less than 3 Å, $H_{N\epsilon}$ and O_{alc} are in hydrogen bond distance, which is prerequisite to catalytic activity. Binding mode I was therefore assumed to be productive. For the fast-reacting as well as for the slow-reacting enantiomer, the large hydrophobic substituent was placed in the hydrophobic dent. For the fast-reacting enantiomer the medium-sized substituent was placed at the entrance to the hydrophilic trench with the hydrogen atom at the stereocenter pointing toward the rigid oxyanion stop of the lipase. For the slow-reacting enantiomer, the medium-sized substituent and the hydrogen switch (Nakamura et al., 1994). The medium-sized substituent points toward the oxyanion stop of the lipase, thus causing strong sterical repulsion

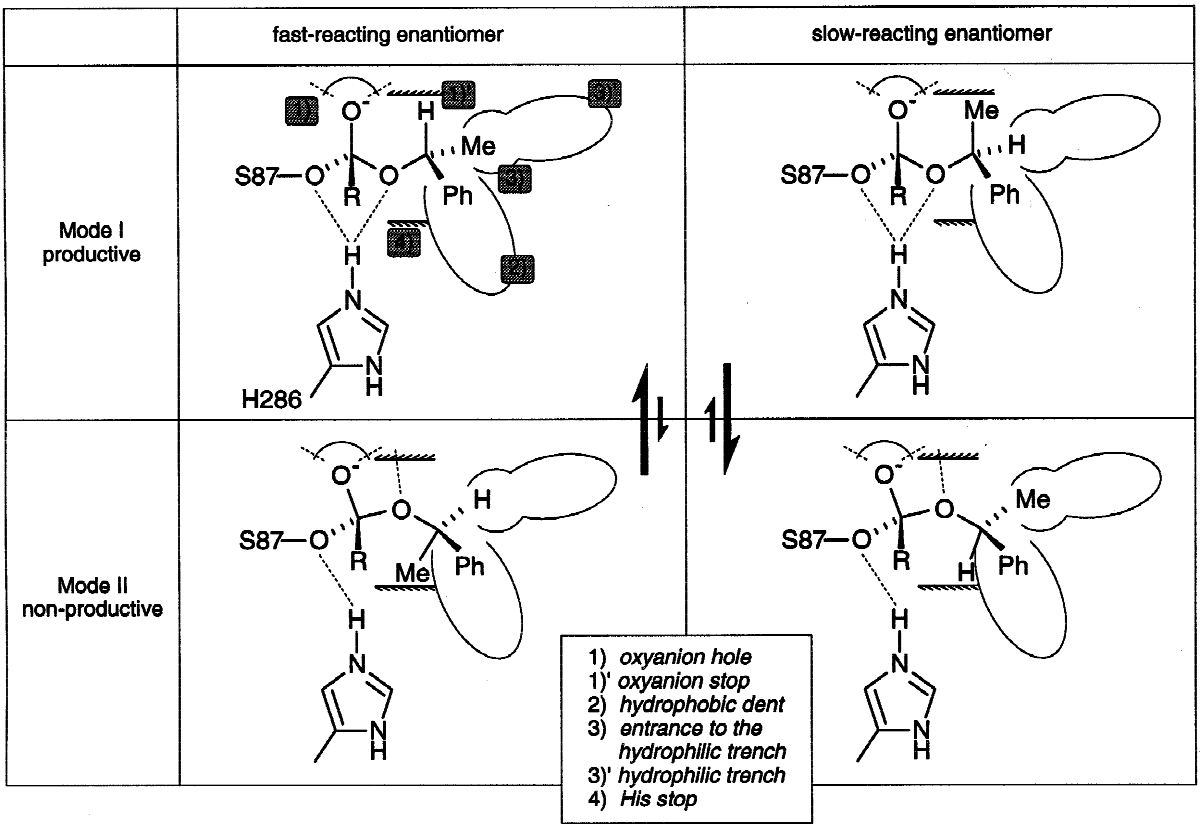

Fig. 4. Binding pockets and binding modes for each case of fast- and slow-reacting enantiomers in *P. cepacia* lipase including essential hydrogen bonds (—) and repulsive interactions between medium-sized substituents of the alcohol moiety of substrates and rigid parts of the lipase: the oxyanion stop and the His stop. The entrance of the hydrophilic trench is separated from the hydrophilic trench by a contradiction composed of side chains of residues Y29 and L287. The large and medium-sized substituent are represented by phenyl and methyl, respectively.

between lipase and substrate. This high potential energy was concluded to result in a low equilibrium concentration of the slow-reacting enantiomer in productive mode I and thus explains experimentally observed stereopreference.

Binding mode II (nonproductive)

Binding mode II is characterized by a distance $d(\mathrm{H}_{N\epsilon} - \mathrm{O}_{alc})$ longer than 3 Å and thus was assumed to be nonproductive. As in mode I, for both enantiomers the hydrophobic dent accommodates the large, hydrophobic substituent of the secondary alcohol moiety. In contrast to mode I, the medium-sized substituent of the slow-reacting enantiomer points toward the entrance of the hydrophilic trench and the hydrogen atom at the stereocenter points toward the rigid His stop of the lipase. In mode II, repulsive interactions were observed for the fast-reacting enantiomer, where the medium-sized substituent was pointing toward the rigid His stop. These interactions were probably the reason for a conformational change, which occurred during simulations of fast-reacting enantiomers of all substrates: starting structures of fast-reacting enantiomers, docked in nonproductive mode II, underwent a conformational change during molecular dynamics simulations to an orientation close to productive mode I. We concluded that the equilibrium concentration of fast-reacting enantiomer in binding mode II should be low.

For all fast-reacting enantiomers, the optimal binding mode is represented by the productive mode I, while the optimal binding mode for the slow-reacting enantiomers is nonproductive mode II.

A third binding mode?

A third binding mode could be possible, where the large substituent at the stereocenter points toward the hydrophilic trench. While medium-sized substituents only reach the entrance to the hydrophilic trench, most of the large substituents are large enough to be accommodated by the hydrophilic trench. However, this binding mode led to unfavorable interactions of large hydrophobic substituents with the hydrophilic bottom of the hydrophilic trench. Therefore, we concluded this binding mode to be less populated in the reaction equilibrium, and we did not consider this third binding mode in further investigations of enantioselectivity.

Identification of a crucial geometrical parameter $d(H_{N\epsilon} - O_{alc})$ and correlation to experimental enantioselectivity

Substrates were covalently docked to the side-chain oxygen of catalytic S87, and molecular dynamics simulations were performed. The distance $d(\mathrm{H}_{N\epsilon} - \mathrm{O}_{alc})$ between the hydrogen atom of catalytic H286 and the oxygen of the alcohol moiety was selected

as crucial geometrical parameter and was analyzed for each binding mode. It is a crucial geometrical parameter for enzymatic hydrolysis, because it promotes the collapse of the first tetrahedral intermediate (Fig. 1) by a fast hydrogen transfer and, therefore, the cleavage of the ester. For enzymatic esterification, it promotes the formation of the second tetrahedral intermediate (Fig. 1).

Fast-reacting enantiomers in productive binding mode I

Distances $d(H_{N\epsilon} - O_{alc})$ for fast-reacting enantiomers had an average value of 2.5 Å (mean-square deviation ± 0.2 Å). The smallest and largest values were 2.0 and 2.9 Å, respectively. A single outlier shows a distance shorter than 2.0 Å. A short distance $d(H_{N\epsilon} - O_{alc})$ for fast-reacting enantiomers should promote a fast conversion, and thus result in high enantioselectivity. However, no correlation was observed for fast-reacting enantiomers (Fig. 5A), because for most substrates the distance $d(H_{N\epsilon} - O_{alc})$ is about 2.5 Å and was not correlated to experimentally determined enantioselectivities. This made the analysis of $d(H_{N\epsilon} - O_{alc})$ in productive mode I less appropriate for a prediction of enantioselectivity.

Slow-reacting enantiomers in productive binding mode I

Distances $d(H_{N\epsilon} - O_{alc})$ for slow-reacting enantiomers had an average value of 2.3 ± 0.3 Å. The extreme values were 1.6 and 3.2 Å. Correlation of this parameter showed a clear trend in all regions of enantioselectivity (Fig. 5B): substrates with low enantioselectivity ($E \leq 20$) resulted in distances of $d(H_{N\epsilon} - O_{alc}) \leq$ 2.0 Å, and substrates with high enantioselectivity ($E \geq 100$) resulted in distances of $d(H_{N\epsilon} - O_{alc}) \geq 2.2$ Å. The twilight zone, which includes substrates of low, medium, and high enantioselectivity, was limited to a narrow zone between 2.0 and 2.2 Å. Dis-

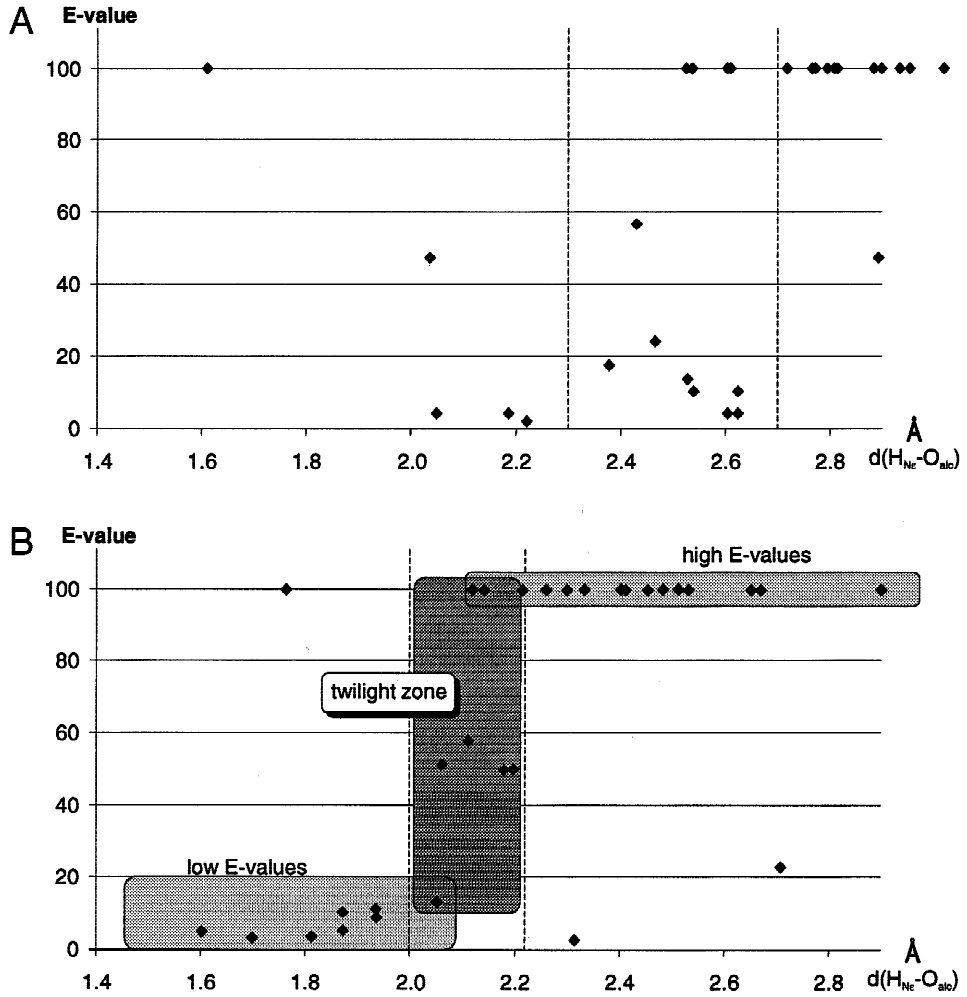

Fig. 5. A: Correlation of the distance $d(H_{N\epsilon} - O_{alc})$ of fast-reacting enantiomers in productive mode I to experimentally determined E values. E values > 100 were displayed at the ordinate at $E = 100$. The mean-square deviation (2.5 ± 0.2 Å) is indicated. Strong correlation is not observed for fast-reacting enantiomers, because for most substrates the distance $d(H_{N\epsilon} - O_{alc})$ is about 2.5 Å and not correlated to experimentally determined enantioselectivities. **B:** Correlation of the distance $d(H_{N\epsilon} - O_{alc})$ of slow-reacting enantiomers in productive mode I to experimentally determined E values. E values > 100 were displayed at the ordinate at $E = 100$. Substrates were classified into three categories of enantioselectivity: substrates with low enantioselectivity ($E < 20$) show distances $d(H_{N\epsilon} - O_{alc}) < 2.1$ Å and substrates with high enantioselectivity ($E = 100$) show distances $d(H_{N\epsilon} - O_{alc}) > 2.1$ Å. The twilight zone includes substrates of low, medium, and high enantioselectivity, and is limited to a zone of 0.2 Å (2.0 to 2.2 Å). The three outliers are shaded gray in Figure 1.

tances $d(H_{N\epsilon} - O_{alc}) \leq 2.0$ Å in slow-reacting enantiomers promote a fast conversion of slow-reacting enantiomers, and therefore slow- and fast-reacting enantiomers were assumed to be converted at similar rates, resulting in a decrease of enantioselectivity. A distance $d(H_{N\epsilon} - O_{alc}) \geq 2.2$ Å, however, is preventing efficient catalysis of slow-reacting enantiomers and facilitates high enantioselectivity.

Three out of 30 investigated substrates failed in the correlation. These substrates have in common a polar 4-OCH_3Ph group at the large substituent (shaded in gray in Fig. 2), which is at least five atoms away from the stereocenter, whereas none of the other substrates have a polar group in this position.

Nonproductive binding mode II

Due to strong sterical repulsion, the nonproductive mode II was not observed for fast-reacting enantiomers. For slow-reacting enantiomers, the distance $d(H_{N\epsilon} - O_{alc})$ laid beyond 3.5 Å and was too far to allow formation of a productive hydrogen bond between $H_{N\epsilon}$ of catalytic histidine and the alcohol oxygen. However, the alcohol oxygen of the substrate in nonproductive mode II is stabilized by residue L17, and the oxyanion is hydrogen bonded to L17 and Q88. Therefore, tetrahedral intermediates of slow-reacting enantiomers are stabilized without repulsive interactions. This mode was assumed to be highly populated in the reaction equilibrium of slow-reacting enantiomers.

Discussion

Substrates

Stereopreference toward chiral secondary alcohols has been reliably predicted by the structure of the secondary alcohol moiety (Kazlauskas et al., 1991). However, the atomic details of factors that mediate enantioselectivity are largely obscure, and there is no general quantitative correlation between structure and enantioselectivity like "the larger the *L* and the smaller the *M*, the higher enantioselectivity *E*": *E* has been shown to be high for $M = CH_3$ and $L = C_6H_5$, but low for the more bulky $L = C_6H_4$-*p*(OCH_3) (Laumen & Schneider, 1988); for $L = CH{=}CHC_6H_5$ and $M = CO_2H$, enantioselectivity *E* is medium (Chadha & Manohar, 1995), but for the bigger $M = CO_2CH_2CH_3$ enantioselectivity *E* is high (Bornscheuer et al., 1993). It is therefore necessary to include the alcohol binding pocket of the biocatalyst into the model. We have selected 30 secondary alcohols from over 100 experimentally investigated examples (Kazlauskas & Bornscheuer, 1998), ranging from low enantioselectivity ($E = 20$) to high enantioselectivity ($E = 100$). Only substrates consisting of C, H, N, O, and halogen atoms were selected, because these atoms are most reliably parameterized in molecular dynamics force fields. As a further criterion, substrates varied over a broad range of size, shape, and physicochemical properties of substituents at the stereocenter: medium-sized substituents ranged from small, spherical, and hydrophobic (e.g., $-CH_3$) to larger and more hydrophilic substituents (e.g., $-CO_2CH_3$), large substituents were saturated and unsaturated aliphatic as well as aromatic substituents, including three rigid cyclic systems (Fig. 2).

Docking

Alcohol moieties include at least three rotatable bonds; therefore, the conformational space of the alcohol moiety is large. However, flexibility is restricted due to two well-defined binding pockets within the active site of the lipase, the hydrophobic dent and the entrance to the hydrophilic trench, and two rigid stops, the oxyanion stop and the His stop.

Comparison of X-ray structures of free (Schrag et al., 1997) and inhibited *P. cepacia* lipase (Lang et al., 1998) has shown that backbone atoms do hardly move upon substrate binding (Cα root-mean-square 0.4 Å), and thus follow the lock and key model (Fischer, 1894), while side chains reorientate and show induced fit behavior (Koshland & Thoma, 1960). Accordingly, we performed molecular dynamics simulations by constraining the position of backbone atoms and allowing the side chains and the substrate to move.

Two binding modes, a productive and a nonproductive one, were identified, which differed in the distance $d(H_{N\epsilon} - O_{alc})$. Which binding mode is preferentially populated by each enantiomer depends on sterical and physico-chemical properties of the substituents. For both modes, the large substituent was situated in the hydrophobic dent, whereas for the medium-sized substituent there were two possibilities where it could be accommodated—in the entrance to the hydrophilic trench or directing toward either of two rigid lipase stops, which then led to atomic clashes. This occurred for fast-reacting enantiomers in nonproductive mode II and for slow-reacting enantiomers in productive mode I. We assumed that these repulsive interactions are the reason for a high population of fast-reacting enantiomers in productive and slow-reacting enantiomers in the nonproductive mode.

Our model is supported by X-ray structures of *C. rugosa* lipase complexes with either enantiomer of menthyl hexylphosphonate (Cygler et al., 1994). The analogue of the fast-reacting enantiomer was bound in productive mode (distance $d(N\epsilon - O_{alc})$ 3.1 Å), while the analogue of the slow-reacting enantiomer was bound in a nonproductive binding mode (distance $d(N\epsilon - O_{alc})$ 4.4 Å). The analogue of the slow-reacting enantiomer distorted the orientation of the imidazole ring of catalytic histidine and broke the hydrogen bond between the imidazole and the oxygen of the menthyl. This is in accordance with our observation of the side-chain flexibility of catalytic H286 in *P. cepacia* lipase upon binding of slow-reacting enantiomers, where the imidazole ring flipped toward the side chains of V266 and V267. This resulted in an increase in the distance $d(H_{N\epsilon} - O_{alc})$, which explains a slow conversion of slow-reacting enantiomers.

Investigations of stereopreference in lipase-catalyzed conversion of secondary alcohols and of lipase binding sites have been performed (Kazlauskas, 1994). This model also argued with binding of substituents to well-defined binding pockets. The binding site that accommodates the medium-sized ligand was called the M_L region and is identical to the entrance to the hydrophilic trench. This pocket was identified as crucial for discriminating between medium-sized and large substituents. The model also reported rigid parts, which limit the size of the binding site—the His loop and the oxyanion loop, which are identical to His stop and oxyanion stop in our model. The importance of restrictions of the lipase binding site by residues of the oxyanion hole and the imidazole ring have also been observed for *C. rugosa* lipase (Zuegg et al., 1997), where residues of the oxyanion hole restrict the available space in such a way that only a hydrogen atom fits in. Therefore, the hydrogen of the asymmetric carbon always directed to the same site and both enantiomers were investigated in a productive binding mode.

However, the importance of considering different binding modes have been pointed out in a modeling study of *C. antarctica* lipase

B (Haeffner et al., 1998). The two enantiomers of a secondary alcohol were shown to bind in two different orientations, and the binding modes were classified as productive and nonproductive due to the distance $d(H_{N\epsilon} - O_{alc})$. Free energy calculations have shown an energetically preferred population of productive mode by fast-reacting enantiomers and of nonproductive mode by slow-reacting enantiomers. In many cases, trapping of slow-reacting enantiomers in productive mode resulted in a nonactive hydrogen bond pattern.

Scoring

Although previously reported models allow a correct prediction of stereopreference, they fail in the quantitative prediction of stereoselectivity. In this work we deflect from energy calculations and focus on a new scoring strategy, which is exclusively based on geometrical parameters of substrate–lipase complexes. Quantum-chemical methods (Hu et al., 1998; Monecke et al., 1998) have identified the tetrahedral substrate–lipase complex and the catalytically important distance $d(H_{N\epsilon} - O_{alc})$ as crucial to catalytic activity. Since the ratio between lipase activity (Nakamura et al., 1996; Nishizawa et al., 1997) toward fast- and slow-reacting enantiomers results in experimentally observable enantioselectivity ($E = (k_{cat}/K_m)_{fast}/(k_{cat}/K_m)_{slow}$), the hydrogen-bonding network (Ema et al., 1998) above all the distance $d(H_{N\epsilon} - O_{alc})$ for both enantiomers should be relevant to enantioselectivity. Because distances $d(H_{N\epsilon} - O_{alc})$ of fast-reacting enantiomers were about 2.5 Å for most of investigated substrates with less variation, we focused on distances $d(H_{N\epsilon} - O_{alc})$ of slow-reacting enantiomers. This in accordance with kinetic studies (Ema et al., 1998), which demonstrated that differences in the conversion of both enantiomers do not result from enhanced reactivity of fast-reacting enantiomers but from reduced reactivity of slow-reacting enantiomers.

An appropriate orientation of catalytic H286 in slow-reacting enantiomers should accelerate hydrogen transfer and lead to a decrease in enantioselectivity. The correlation (Fig. 5B) of the identified structural parameter $d(H_{N\epsilon} - O_{alc})$ of slow-reacting enantiomers in productive mode I showed good correlation of calculated and experimental data, and allowed a correct allocation of 27 of 30 investigated substrates into three categories of enantioselectivity.

Outliers—A third binding mode?

Three secondary alcohols (shaded grey in Fig. 2) fail in the correlation to experimentally determined enantioselectivity. These three substrates have in common a polar group (4-OCH_3Ph) at the large substituent, at least five atoms away from the stereocenter. In other alcohols, which correlate, polar residues at the large substituents are situated closer to the stereocenter. In our model, the large substituent always situated in the hydrophobic dent. While polar residues close to the stereocenter are situated near the polar side-chain imidazole of catalytic H286, polar residues, which are more than five atoms away from the stereocenter reach far into the hydrophobic dent and are close to hydrophobic residues of L248, V266, and L287. For the three substituents, which did not fit to our model, a third binding mode could be possible, where the large substituent binds to the hydrophilic trench for both enantiomers, and the polar residue at the large substituent is close to polar residues T18, E28, Y29, and Q292.

The model

The model avoids energy calculation (Norin et al., 1993, 1994; Haeffner et al., 1998) and is exclusively based on structural properties of tetrahedral intermediates. As previous works have already shown, the applied docking methods are reliable and sufficiently precise to correctly predict stereopreference (Scheib et al., 1998, 1999). However, problems occur currently in the application of scoring strategies, which are general enough to predict substrate ranking. Therefore, our model is based on common docking methods, but includes a new approach of structure-based scoring strategy.

In our model, experimentally determined enantioselectivity was always selected from most optimized experimental reaction conditions. Solvent engineering studies of *P. cepacia* lipase have shown that solvent can contribute significantly to enantioselectivity: conversion of a secondary alcohol (Fig. 2: $M = CF_3$, L = naphthyl) showed low enantioselectivity ($E = 22$) in t-butyl methyl ether, medium enantioselectivity ($E = 60$–70) in diethyl ether, toluene, dodecane, and hexane, and high enantioselectivity ($E > 100$) in tetrahydrofuran, acetone, and benzene (Gaspar & Guerrero, 1995). In other cases, however, solvent had no effect on enantioselectivity (Petschen et al., 1996): enantioselectivity for $M = CF_3$ and $L = C_{12}H_{25}$ (Fig. 2) could not be increased above $E = 13$ in hexane, tetrahydrofuran, benzene, acetone, diethyl ether, CH_2Cl_2, CH_3Cl, vinyl acetate, and toluene. These observations suggest that increasing enantioselectivity by solvent engineering is limited by the structure of lipase and secondary alcohol. If based on the structure, the two enantiomers are well differentiated by the lipase, using optimal solvent results in high enantioselectivity, while using suboptimal solvent decreases enantioselectivity. If, however, the structure-based enantioselectivity between lipase and substrate is low, solvent engineering is not expected to be able to increase enantioselectivity above this limit.

Protein engineering offers a way to increase enantioselectivity beyond these limits by modifying sequence and structure of the lipase. Thus, the model might be used to predict mutants of *P. cepacia* lipase with increased enantioselectivity toward secondary alcohols.

Conclusion

In the present study, a simple and general model was presented, which allows the classification of secondary alcohols in *P. cepacia* lipase-catalyzed conversion into three categories of enantioselectivity: zones for low and high enantioselectivity, separated by a narrow twilight zone. The values of a single geometrical parameter, the distance $d(H_{N\epsilon} - O_{alc})$, of the tetrahedral substrate–lipase intermediates of 27 of 30 selected substrates served as an indicator for enantioselectivity and correlated well with experimentally determined enantioselectivity. Based on this study, it is possible to predict enantioselectivity of *P. cepacia* lipase toward a broad range of secondary alcohols by performing molecular dynamics simulations.

Materials and methods

Molecular modeling

Hard- and software

Molecular modeling studies were carried out on Silicon Graphics Workstations Indigo2/R10000. The software for energy mini-

mization and molecular dynamics simulations was Sybyl 6.3 and Sybyl 6.5 (Tripos, St. Louis, Missouri) using the Tripos force field (Clark et al., 1989). Docking of substrates was performed with the commercial docking tool FlexX (Rarey et al., 1996).

Molecular dynamics simulations

X-ray structures were obtained from the Protein Data Bank (PDB) (Bernstein et al., 1977). The structure of the open form of *P. cepacia* lipase (Schrag et al., 1997) has been taken from the PDB (PDB entry 3lip) and the water molecules were removed. Docking was guided by the crystal structure of *P. cepacia* lipase complexed with the substrate analogues inhibitors (R_P,S_P)-1,2-dioctylcarbamoylglycero-3-O-p-nitrophenyl octylphosphonate (PDB entry 5lip) (Lang et al., 1998). Covalently docked substrates mimicked the first tetrahedral transition state, which is the rate-limiting step of lipase-catalyzed hydrolysis of esters of secondary alcohols. The oxyanion was oriented to the oxyanion hole (L17 and Q88) and the tetrahedral carbon of the substrate was covalently linked to the side-chain oxygen Oγ of catalytic S87. The acid chain was docked to the hydrophobic crevice (Scheib et al., 1998). Docking of the alcohol moiety was performed with FlexX. Because FlexX keeps the receptor fixed during docking, large alcohol moieties could not be docked into the binding site of uninhibited *P. cepacia* lipase as taken from the PDB. To circumvent manual docking and to enable FlexX, we performed substrate docking within an enlarged binding site. Therefore, a single selected substrate with large substituents was manually modeled into the binding site of *P. cepacia* lipase, covalently linked to Oγ of catalytic serine, and molecular dynamics simulations were performed. An average structure was created by superimposing and averaging 25 substrate–lipase structures of the production phase, and the substrate was removed. This structure with the enlarged binding site was used as template for further substrate dockings using FlexX. Appropriate docking structures must show an active hydrogen bond pattern.

Because the substrate–lipase complex mimics the first transition state of the lipase catalyzed hydrolysis of esters of secondary alcohols, the protonation state at H286 and the partial charges of S87, H286, and the substrate were modified (Holzwarth et al., 1997) as calculated by the semiempirical method MNDO94/PM3 (Stewart, 1989).

The structures of the substrate–lipase complexes were refined by energy minimization and subsequent molecular dynamics simulations (Holzwarth et al., 1997). Energy minimization and molecular dynamics simulations were carried out in vacuo with constrained protein backbone. During the initial equilibration phase, the complexes were equilibrated in three intervals of 1 ps at 5, 30, and 70 K, and 4 ps at 100 K, followed by a production phase of 1 ps at 100 K. The step size was 1 fs up to 30 K and 0.5 fs for 70 and 100 K. The nonbonded interaction cutoff was set to 8 Å, the coupling constant to 10 fs, and the dielectric constant to 1.0. Conformers were saved every 40 fs. An average structure was created by superimposing and averaging 25 substrate–lipase complex structures of the production phase. The average structures were analyzed by measuring $d(H_{N\epsilon} - O_{alc})$.

Selection of experimental data

Published experimental enantioselectivities differed over a wide range and depended on experimental conditions such as solvent, temperature, additives, and many other effects. To correlate $d(H_{N\epsilon} - O_{alc})$ to enantioselectivity E, the most optimized published enantioselectivities were selected. In cases of asymmetric synthesis, where E values generally are given for only one reaction condition, we assumed that such reactions had been optimized with regard to enantioselectivity.

Acknowledgments

We thank Aventis Research & Technologies for financial support.

References

Bänziger M, Griffiths GJ, McGarrity JF. 1993. A facile synthesis of (2R,3E)-4-iodobut-3-en-2-ol and (2S,3E)-4-iodobut-3-en-2-yl chloroacetate. *Tetrahedron: Asymmetry 4*:723–726.

Bemis GW, Carlson-Golab G, Katzenellenbogen JA. 1992. A molecular dynamics study of the stability of chymotrypsin acyl enzymes. *J Am Chem Soc 114*:570–578.

Bernstein FC, Koetzle TF, Williams GJB, Meyer EF Jr, Brice MD, Rodgers JR, Kennard O, Shimanouchi T, Tasumi M. 1977. The Protein Data Bank: A computer-based archival file for macromolecular structures. *J Mol Biol 112*:525–542.

Bornscheuer UT, Herar A, Kreye L, Wendel V, Capewell A. 1993. Factors affecting the lipase catalyzed transesterification reactions of 3-hydroxy esters in organic solvents. *Tetrahedron: Asymmetry 4*:1007–1016.

Burgess K, Jennings LD. 1991. Enantioselective esterifications of unsaturated alcohols mediated by a lipase prepared from *Pseudomonas sp. J Am Chem Soc 113*:6129–6139.

Caron G, Kazlauskas RJ. 1991. An optimized sequential kinetic resolution of *trans*-1,2-cyclohexanediol. *J Org Chem 56*:7251–7256.

Chadha A, Manohar M. 1995. Enzymatic resolution of 2-hydroxy-4-phenylbutanoic acid and 2-hydroxy-4-phenylbutenoic acid. *Tetrahedron: Asymmetry 6*:651–652.

Chapus C, Sémériva M. 1976. Mechanism of pancreatic lipase action. 2. Catalytic properties of modified lipases. *Biochemistry 15*:4988–4991.

Chapus C, Sémériva M, Bovier-Lapierre C, Desnuelle P. 1976. Mechanism of pancreatic lipase action. 1. Interfacial activation of pancreatic lipase. *Biochemistry 15*:4980–4987.

Clark M, Cramer RD III, van Opdenbosch N. 1989. Validation of the general purpose TRIPOS 5.2 force field. *J Comp Chem 10*:982–1012.

Cygler M, Grochulski P, Kazlauskas RJ, Schrag JD, Bouthillier F, Rubin B, Serreqi AN, Gupta AK. 1994. A structural basis for the chiral preferences of lipases. *J Am Chem Soc 116*:3180–3186.

DeTar DF. 1981. Computation of enzyme-substrate specificity. *Biochemistry 20*:1730–1743.

Ema T, Kobayashi J, Maeno S, Sakai T, Utaka M. 1998. Origin of the enantioselectivity of lipases explained by a stereo-sensing mechanism operative at the transition state. *Bull Chem Soc Jpn 71*:443–453.

Faber K, Griengl H, Hönig H, Zuegg J. 1994. On the prediction of the enantioselectivity of *Candida rugosa* lipase by comparative molecular field analysis. *Biocatalysis 9*:227–239.

Fischer E. 1894. Einfluss der Configuration auf die Wirkung der Enzyme. *Ber Dt Chem Ges 27*:2985–2993.

Gaspar J, Guerrero A. 1995. Lipase-catalysed enantioselective synthesis of napthyl trifluoromethyl carbinols and their corresponding non-fluorinated counterparts. *Tetrahedron: Asymmetry 6*:231–238.

Haeffner F, Norin T, Hult K. 1998. Molecular modeling of the enantioselectivity in lipase-catalyzed transesterification reactions. *Biophys J 74*:1251–1262.

Hamada H, Shiromoto M, Funahashi M, Itoh T, Nakamura K. 1996. Efficient synthesis of optically pure 1,1,1-trifluoro-2-alkanols through lipase-catalyzed acylation in organic media. *J Org Chem 61*:2332–2336.

Holzwarth HC, Pleiss J, Schmid RD. 1997. Computer aided modelling of *Rhizopus oryzae* lipase catalyzed stereoselective hydrolysis of triglycerides. *J Mol Catal B: Enzymatic 3*:73–82.

Hönig H, Shi N, Polanz G. 1994. Enzymatic resolutions of heterocyclic alcohols. *Biocatalysis 9*:61–69.

Hu CH, Brinck T, Hult K. 1998. Ab initio and density functional theory studies of the catalytic mechanism for ester hydrolysis in serine hydrolases. *Int J Quantum Chem 69*:89–103.

Itoh T, Hiyama Y, Betchaku A, Tsukube H. 1993. Enhanced reaction rate and enantioselectivity in lipase-catalyzed hydrolysis by addition of a crown ether. *Tetrahedron Lett 34*:2617–2620.

Kaminska J, Gornicka I, Sikora M, Gora J. 1996. Preparation of homochiral (S)- and (R)-1-(2-furyl)ethanols by lipase-catalyzed transesterification. *Tetrahedron: Asymmetry 7*:907–910.

Kazlauskas RJ. 1994. Elucidating structure-mechanism relationships in lipases: Prospects for predicting and engineering catalytic properties. *Trends Biotechnol 12*:464–472.

Kazlauskas RJ, Bornscheuer UT. 1998. Biotransformations with lipases In: Rehm HJ, Reed G, Pühler A, Stadler PJW, Kelly DR, eds. *Biotransformations with lipases in biotechnology*, Vol. 8. Weinheim, Germany: VCH. pp 37–191.

Kazlauskas RJ, Weissfloch ANE, Rappaport T, Cuccia LA. 1991. A rule to predict which enantiomer of a secondary alcohol reacts faster in reactions catalyzed by cholesterol esterase, lipase from *Pseudomonas cepacia*, and lipase from *Candida rugosa*. *J Org Chem 56*:2656–2665.

Koshland DE, Thoma JA. 1960. Competitive inhibition by substrate during enzyme action. Evidence for the induced-fit theory. *J Am Chem Soc 82*:3329–3333.

Lang DA, Mannesse ML, de Haas GH, Verheij HM, Dijkstra BW. 1998. Structural basis of the chiral selectivity of *Pseudomonas cepacia* lipase. *Eur J Biochem 254*:333–340.

Laumen K, Schneider MP. 1988. A highly selective ester hydrolase from *Pseudomonas* Sp. for the enzymatic preparation of enantiomerically pure secondary alcohols, chiral auxiliaries in organic synthesis. *J Chem Soc Chem Commun* 598–600.

Liang S, Paquette LA. 1990. Biocatalytic-based synthesis of optically-pure (C-6)-functionalized 1-(tert-butyldimethylsilyloxy) 2-methyl-(E)-2-heptenes. *Tetrahedron: Asymmetry 1*:445–452.

Monecke P, Friedemann R, Naumann S, Csuk R. 1998. Molecular modelling studies on the catalytic mechanism of *Candida rugosa* lipase. *J Mol Model 4*:395–404.

Naemura K, Fukuda R, Konishi M, Hirose K, Tobe Y. 1994. Lipase YS catalyzed acylation of alcohols: A predictive active site model for lipase YS to identify which enantiomer of a primary or secondary alcohol reacts faster in this acylation. *Chem Soc Perkin Trans I*:1253–1256.

Naemura K, Fukuda R, Murata M, Konishi M, Hirose M, Tobe Y. 1995. Lipase YS-catalyzed enantioselective acylation of alcohols: A predictive active site model for lipase YS to identify which enantiomer of an alcohol reacts faster in this acylation. *Tetrahedron: Asymmetry 6*:2385–2394.

Nakamura K, Kawasaki M, Ohno A. 1994. Effects of substrate structure on lipase-catalyzed transesterification of ω-substituted 1-alkanols in organic solvents. *Bull Chem Soc Jpn 67*:3053–3056.

Nakamura K, Kawasaki M, Ohno A. 1996. Lipase-catalyzed transesterification of aryl-substituted alkanols in an organic solvent. *Bull Chem Soc Jpn 69*:1079–1085.

Nishizawa K, Ohgami Y, Matsuo N, Kisida H, Hirohara H. 1997. Studies on hydrolysis of chiral, achiral and racemic alcohol esters with *Pseudomonas cepacia* lipase: Mechanism of stereospecificity of the enzyme. *J Chem Soc Perkin Trans 2*:1293–1298.

Norin M, Haeffner F, Achour A, Norin T, Hult K. 1994. Computer modeling of substrate binding to lipases from *Rhizomucor miehei, Humicola lanuginosa,* and *Candida rugosa*. *Protein Sci 3*:1493–1503.

Norin M, Hult K, Mattson A, Norin T. 1993. Molecular modeling of chymotrypsin–substrate interactions: Calculation of enantioselectivity. *Biocatalysis 7*:131–147.

Orrenius C, van Heusden C, van Ruiten J, Overbeeke PLA, Kierkels H, Duine JA, Jongejan JA. 1998. Simple conformation space search protocols for the evaluation of enantioselectivity of lipases. *Protein Eng 11*:1147–1153.

Partali V, Waagen V, Alvik T, Anthonsen T. 1993. Enzymatic resolution of butanoic esters of 1-phenylmethyl and 1-[2-phenylethyl]ethers of 3-chloro-1,2-propanediol. *Tetrahedron: Asymmetry 4*:961–968.

Petschen I, Malo EA, Bosch MP, Guerrero A. 1996. Highly enantioselective synthesis of long chain alkyl trifluoromethyl carbinols and β-thiotrifluoromethyl carbinols through lipases. *Tetrahedron: Asymmetry 7*:2135–2143.

Rarey M, Kramer B, Lengauer T, Klebe G. 1996. A fast flexible docking method using an incremental construction algorithm. *J Mol Biol 261*:470–489.

Rotticci D, Orrenius C, Hult K, Norin T. 1997. Enantiomerically enriched bifunctional sec-alcohols prepared by *Candida antarctica* lipase B catalysis. Evidence of non-steric interactions. *Tetrahedron: Asymmetry 8*:359–362.

Scheib H, Pleiss J, Kovac A, Paltauf F, Schmid RD. 1999. Stereoselectivity of Mucorales lipases toward triradylglycerols—A simple solution to a complex problem. *Protein Sci 8*:215–221.

Scheib H, Pleiss J, Schmid RD. 1998. Rational design of *Rhizopus oryzae* lipase with modified stereoselectivity toward triradylglycerols. *Protein Eng 11*: 675–682.

Schneider MP, Georgens U. 1992. An efficient route to enantiomerically pure antidepressants: Tomoxetine, nisoxetine and fluoxetine. *Tetrahedron: Asymmetry 3*:525–528.

Schrag JD, Li Y, Cygler M, Lang DA, Borgdorf T, Schmid HJ, Hecht R, Schomburg D, Rydel T, Oliver J, et al. 1997. The open conformation of a *Pseudomonas lipase*. *Structure 5*:187–202.

Shimizu M, Kawanami H, Fujisawa T. 1992. A lipase-mediated asymmetric hydrolysis of 3-acyloxy-1-octynes and 3-(E)-acyloxy-1-octenes. *Chem Lett* 107–110.

Stewart JJP. 1989. Optimization of parameters for semiempirical methods. *J Comp Chem 10*:209–220.

Takagi Y, Teramoto J, Kihara H, Itoh T, Tsukube H. 1996. Thiacrown ether as regulator of lipase-catalyzed trans-esterification in organic media—Practical optical resolution of allyl alcohols. *Tetrahedron Lett 37*:4991–4992.

Takano S, Setoh M, Ogasawara K. 1993. Enantiocomplementary resolution of 4-hydroxy-5-(4-methoxyphenoxy)-1-pentyne using the same lipase. *Tetrahedron: Asymmetry 4*:157–160.

Uejima A, Fukui T, Fukusaki E, Omata T, Kawamoto T. 1993. Efficient kinetic resolution of organosilicon compounds by stereoselective esterification with hydrolases in organic solvent. *Appl Microbiol Biotechnol 38*:482–486.

Waldinger C, Schneider M, Botta M, Corelli F, Summa V. 1996. Aryl propargylic alcohols of high enantiomeric purity via lipase-catalyzed resolutions. *Tetrahedron: Asymmetry 7*:1485–1488.

Zuegg J, Hönig H, Schrag JD, Cygler M. 1997. Selectivity of lipases: Conformational analysis of suggested intermediates in ester hydrolysis of chiral primary and secondary alcohols. *J Mol Catal B Enzymat 3*:83–98.